Int. J. Heat Mass Transfer. Vol. 23, pp. 971–979
Pergamon Press Ltd. 1980. Printed in Great Britain

NUMERICAL SOLUTION TO THE NAVIER–STOKES EQUATIONS FOR LAMINAR NATURAL CONVECTION ABOUT A HORIZONTAL ISOTHERMAL CIRCULAR CYLINDER

T. H. KUEHN
Mechanical Engineering Department and Engineering Research Institute,
Iowa State University, Ames, IA 50010, U.S.A.

and

R. J. GOLDSTEIN
Mechanical Engineering Department, University of Minnesota,
Minneapolis, MN, U.S.A.

(*Received* 10 *September* 1979 *and in revised form* 26 *November* 1979)

Abstract—Laminar natural-convection heat transfer from a horizontal isothermal cylinder is studied by solving the Navier–Stokes and energy equations using an elliptic numerical procedure. Results are obtained for $10^0 \leq Ra \leq 10^7$. The flow approaches natural convection from a line heat source as $Ra \to 0$ and laminar boundary-layer flow as $Ra \to \infty$. Boundary-layer solutions do not adequately describe the flow and heat transfer at low or moderate values of Ra because of the neglect of curvature effects and the breakdown of the boundary-layer assumptions in the region of the plume. Good agreement with experimental results is achieved.

NOMENCLATURE

- D, cylinder diameter;
- g, gravitational acceleration;
- h, local heat-transfer coefficient;
- $\bar{h}$, average heat-transfer coefficient around cylinder;
- k, thermal conductivity of fluid;
- L, radial distance between cylinder surface and outer boundary of solution domain;
- Nu, local Nusselt number, hD/k;
- $\bar{N}u$, average Nusselt number, $\bar{h}D/k$;
- Pr, Prandtl number, ν/α;
- Q, heat transfer from cylinder per unit length, $\bar{h}\pi D(T_w - T_\infty)$;
- R, radial coordinate;
- r, dimensionless radial coordinate, R/D;
- Ra, Rayleigh number, $g\beta D^3(T_w - T_\infty)/\nu\alpha$;
- T, temperature;
- T_w, temperature of cylinder surface;
- T_∞, temperature of ambient fluid;
- U, radial velocity, positive outwards;
- U^*, $UD/\alpha Ra^{1/4}$;
- u, dimensionless radial velocity, UD/α;
- V, angular velocity, positive upward;
- V^*, $VD/\alpha Ra^{1/2}$;
- v, dimensionless angular velocity, VD/α;
- Y, radial distance from cylinder surface;
- Y^*, $YRa^{1/4}/D$.

Greek symbols

- α, thermal diffusivity;
- β, thermal coefficient of volumetric expansion;
- θ, angular coordinate, zero is downward vertical, positive counter-clockwise on right half of cylinder, $0 \leq \theta \leq \pi$;
- ϕ, dimensionless temperature, $(T - T_\infty)/(T_w - T_\infty)$;
- $\Delta\phi$, difference between adjacent dimensionless isotherms;
- ψ, dimensionless stream function;
- $\Delta\psi$, difference between adjacent dimensionless streamlines;
- ω, dimensionless vorticity.

Subscripts

- i, radial grid number;
- j, angular grid number.

INTRODUCTION

NATURAL convection about a single horizontal circular cylinder of uniform temperature suspended in an infinite fluid medium has been studied both experimentally and analytically for several decades [1]. At small Rayleigh numbers the cylinder behaves like a line heat source. Asymptotic matching solutions have been obtained at low Rayleigh numbers by Nakai and Okazaki [2], where an inner conduction-dominated region is matched to an outer region governed mainly by convection.

For moderately large Rayleigh numbers, $10^4 < Ra < 10^8$, the flow is laminar and forms a boundary layer around the cylinder. The assumptions usually made are that curvature effects and the pressure difference across the boundary layer are negligible. Using these assumptions, the simplified boundary-layer equations have been solved using a variety of techniques. Hermann

[3] modified Pohlausen's similarity solution for the vertical flat plate at $Pr = 0.733$. The boundary-layer thickness at different angles around the cylinder was obtained by multiplying the flat-plate boundary-layer thickness by a parameter that is a function only of angle from the stagnation point. The vertical flat-plate boundary-layer solutions given by Ostrach [4] can be used to obtain solutions at other Prandtl numbers. Merk and Prins [5] obtained a similarity solution valid near the stagnation point and later presented an integral solution. Another integral solution was given by Levy [6]. Chiang and Kaye [7] used a Blasius expansion to obtain solutions for cylinders with varying wall temperature at $Pr = 0.7$. A Görtler expansion technique was used by Saville and Churchill [8] to investigate the effect of the Prandtl number. A solution to the transient problem was obtained by Elliott [9] with the results at infinite time given as the steady-state solution. Lin and Chao [10] used a Merk-type series to obtain solutions for various two-dimensional and axisymmetric geometries with the horizontal circular cylinder as a special case. Finite difference solutions have been obtained by Merkin [11, 12] for horizontal circular and elliptic cylinders of uniform temperature or uniform heat flux.

Investigations incorporating curvature effects have been made by Akagi [13], Peterka and Richardson [14] and Gupta and Pop [15]. The curvature effects were found to be small when $Ra > 10^5$ near $Pr = 1$. However, Akagi remarks that for $Pr \ll 1$ or $Pr \gg 1$ curvature effects exist even at a very large Raylcigh number.

The objective of this study is a solution of the complete Navier–Stokes and energy equations for natural convection about a horizontal isothermal circular cylinder. Solutions have been obtained over a wide range in Rayleigh number, $10^0 \leq Ra \leq 10^7$, where neither asymptotic matching techniques nor boundary-layer assumptions are accurate. Results include the development of the buoyant plume which cannot be obtained using boundary-layer methods. The solutions are compared with experimental data for verification.

GOVERNING EQUATIONS

The dimensionless equations for steady, laminar, natural-convection flow can be written in cylindrical polar coordinates using the Boussinesq approximation as follows:

$$\nabla^2\psi = -\omega, \tag{1}$$

$$\nabla^2\omega = \frac{1}{Pr}\left(u\frac{\partial\omega}{\partial r} + \frac{v}{r}\frac{\partial\omega}{\partial\theta}\right) - Ra\left(\sin\theta\frac{\partial\phi}{\partial r} + \frac{\cos\theta}{r}\frac{\partial\phi}{\partial\theta}\right), \tag{2}$$

$$\nabla^2\phi = u\frac{\partial\phi}{\partial r} + \frac{v}{r}\frac{\partial\phi}{\partial\theta} \tag{3}$$

with

$$\nabla^2 = \frac{\partial^2}{\partial r^2} + \frac{1}{r}\frac{\partial}{\partial r} + \frac{1}{r^2}\frac{\partial^2}{\partial\theta^2}. \tag{4}$$

The flow is considered to be symmetric about the vertical plane passing through the center of the cylinder so that the flow on only one side needs to be solved. The boundary conditions become

$$u = v = \psi = 0, \quad \omega = -\frac{\partial^2\psi}{\partial r^2}, \quad \phi = 1 \tag{5}$$

on the impermeable isothermal cylinder surface and

$$v = \psi = \omega = \frac{\partial u}{\partial\theta} = \frac{\partial\phi}{\partial\theta} = 0 \tag{6}$$

on the symmetry lines. The outer boundary must be treated as two parts; one with fluid coming into the solution domain, the other with fluid leaving. The fluid is assumed to approach the cylinder radially at ambient fluid temperature. The inflow boundary conditions are

$$v = \frac{\partial^2\psi}{\partial r^2} = \phi = 0, \quad \omega = -\frac{1}{r^2}\frac{\partial^2\psi}{\partial\theta^2}. \tag{7}$$

The fluid is assumed to leave radially in the plume with negligible radial-temperature gradient. This is a common type of outflow boundary condition providing the velocity is large (i.e. $Pe \gg 1$). The outflow boundary conditions become

$$v = \frac{\partial^2\psi}{\partial r^2} = \frac{\partial\phi}{\partial r} = 0, \quad \omega = -\frac{1}{r^2}\frac{\partial^2\psi}{\partial\theta^2}. \tag{8}$$

SOLUTION TECHNIQUE

A finite-difference overrelaxation method is used to solve the elliptic equations numerically. A central differencing scheme is used for the majority of the solutions although a hybrid technique is used to maintain stability at large Ra. For example, equation (3) can be written in finite difference form as

$$\phi_{i,j} = N_{i,j}\phi_{i+1,j} + S_{i,j}\phi_{i-1,j} + E_{i,j}\phi_{i,j+1} + W_{i,j}\phi_{i,j-1}. \tag{9}$$

The coefficients are calculated as follows:

$$N'_{i,j} = \left[\left[1 + \frac{\Delta r_i}{2r_i} - u_{i,j}\frac{\Delta r_i}{2},\ 0,\ -u_{i,j}\frac{\Delta r_i}{2}\right]\right] \tag{10}$$

where the first term in the brackets is the standard central-difference formulation. Similar expressions are used to obtain $S'_{i,j}$, $E'_{i,j}$ and $W'_{i,j}$. It can be seen from equation (10) that when the velocity is large the central-difference coefficients can become negative leading to divergence in the computations. By taking the largest non-negative term of the three terms in the brackets the coefficients N', S', E' and W' remain positive or zero. The coefficients used in (9) are then obtained as

$$Q = N'_{i,j} + S'_{i,j} + E'_{i,j} + W'_{i,j}, \tag{11}$$

$$N_{i,j} = N'_{i,j}/Q \quad S_{i,j} = S'_{i,j}/Q, \quad E_{i,j} = E'_{i,j}/Q, \quad W_{i,j} = W'_{i,j}/Q. \tag{12}$$

When the velocities are small this scheme reduces to

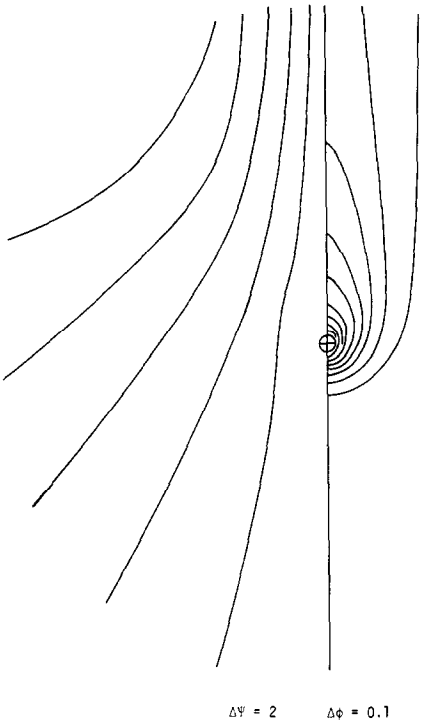

(a) $Ra = 10^0$.

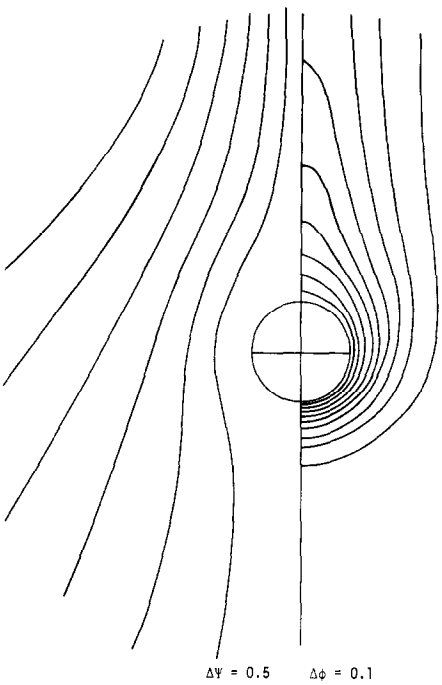

(b) $Ra = 10^2$.

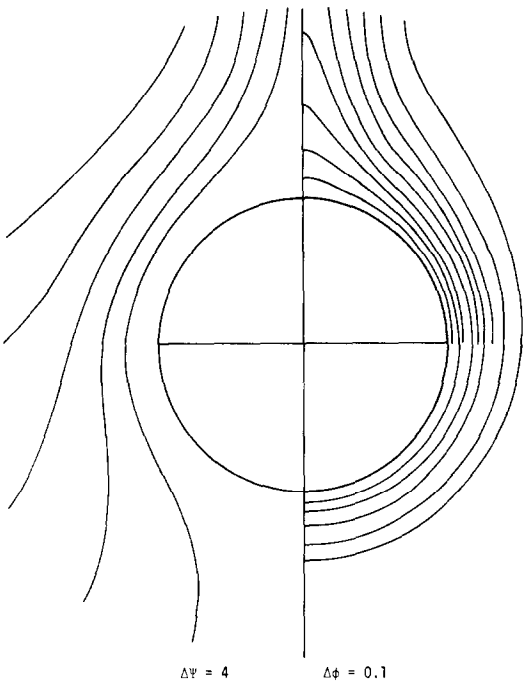

(c) $Ra = 10^4$.

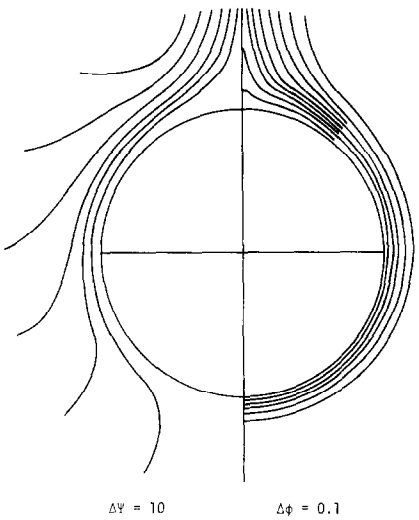

(d) $Ra = 10^6$.

FIG. 1. Streamlines and isotherms at four values of the Rayleigh number, $Pr = 0.7$.

the second-order central-difference formulation.

The radial grid spacing is basically $0.1L$ although this is reduced to as low as $0.0125L$ near the cylinder. The angular grid lines are spaced every 10° except in the region of the plume where a 2.5° angular spacing is used. The position of the outer boundary has an effect on the results if it is not set far enough from the surface of the cylinder. The distance varies from $D \leq L \leq 20D$ depending on the Rayleigh and Prandtl number. Only results from the inner 2/3 of the solution domain are presented since those of the outer 1/3 depend slightly on the location of the outer boundary. The change of

outer-boundary conditions from inflow to outflow is set near $\theta = 150°$, which is near the position of the maximum stream function. Moving 10° either side of this position does not change the results significantly. Further details of the numerical method are given in reference [16].

NUMERICAL RESULTS

Several solutions are obtained at $Pr = 0.7$ over the range $10^0 \leq Ra \leq 10^7$. Stream lines and isotherms from some of these are shown in Fig. 1. The temperature distribution at $Ra = 10^0$ given in Fig. 1(a) resembles what would be found near a line heat source. The flow is basically upward, convecting heat from the cylinder in a well-defined plume. The Rayleigh number is above the range covered by Nakai and Okazaki [2], so a direct comparison is not possible. Analysis of a buoyant plume above a horizontal line heat source indicates that the center line temperature should be proportional to the $-3/5$ power of the distance above some starting point when the plume is fully developed. This has been confirmed experimentally by Schorr and Gebhart [17]. The calculated plume center line temperature for $Ra = 10^0$ and $Pr = 0.7$ is correlated by

$$\phi = 0.80\left(\frac{R}{D}\right)^{-1/2}, \quad \frac{R}{D} \geq 1.5 \tag{13}$$

where R is the vertical distance measured from the center of the cylinder. The same slope correlates the plume center line temperature when $Ra = 10^1$ and 10^2 providing the center of the cylinder is the origin. This indicates that the plume has not reached a fully developed condition in the present solutions.

At larger Rayleigh numbers a boundary layer forms around the cylinder as shown in Fig. 1(c) and 1(d). At $Ra = 10^4$ the boundary-layer thickness is approximately equal to the cylinder radius. The assumption of negligible curvature effect is not valid at this Rayleigh number so the solution to the boundary-layer equations does not give valid results here. However, at $Ra = 10^6$ the boundary-layer thickness has become much thinner than the cylinder radius as shown in Fig. 1(d) so the boundary-layer model should give fairly accurate results. The majority of the flow approaches the cylinder from the side as opposed to the bottom at large Rayleigh numbers. This agrees with the experimental observations of Aihara and Saito [18].

Velocity and temperature distributions at $Ra = 10^5$ and $Pr = 0.7$ are given in Figs. 2–4. The angular velocity distributions shown in Fig. 2 for $30° \leq \theta \leq 150°$ are very similar to what boundary layer solutions predict. However, for $\theta > 150°$ the plume begins to form. The angular velocity drops to zero at $\theta = 180°$. In

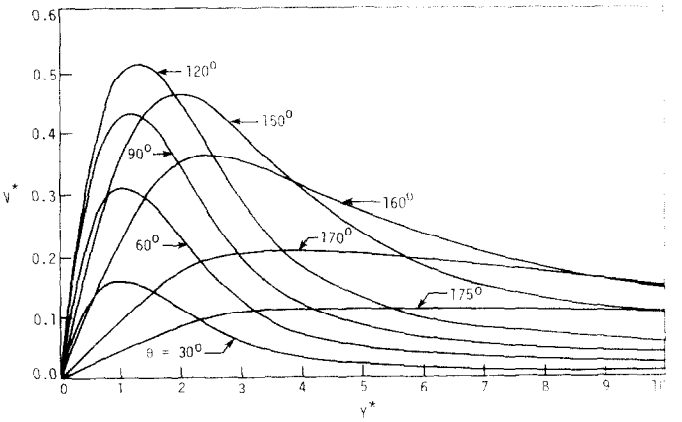

FIG. 2. Angular velocity distribution at $Ra = 10^5$, $Pr = 0.7$.

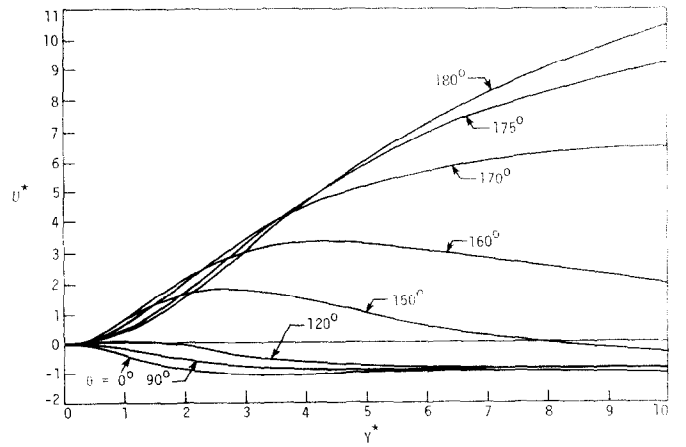

FIG. 3. Radial velocity distribution at $Ra = 10^5$, $Pr = 0.7$.

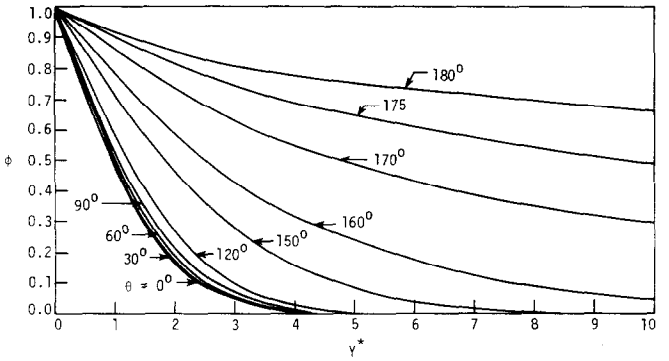

FIG. 4. Temperature distribution at $Ra = 10^5$, $Pr = 0.7$.

the plume, $\theta \simeq 175°$, the angular velocity, or horizontal velocity, is a function only of the horizontal distance from the plume center line and is independent of distance above the cylinder.

Radial velocities are fairly small and uniform around the outer portion of the boundary layer where the flow is moving toward the cylinder. This is shown by the curves for $0° \leq \theta \leq 120°$ in Fig. 3. The flow changes from inflow to outflow between $\theta = 150°$ and $\theta = 160°$. The outflow velocities in the plume are typically an order of magnitude larger than the inflow velocities in the boundary layer. Near the cylinder the vertical velocity in the center of the plume is less than that at $\theta = 175°$. However, for $Y^* > 4.5$ the center line velocity is the largest velocity in the plume. This developing-plume phenomena was found experimentally by Jodlbauer [19] who measured velocities and temperatures at two locations in a plume above a heated horizontal cylinder. A similar velocity distribution has been found in a developing buoyant plume above a heated vertical plate [20].

The temperature distribution at $Ra = 10^5$ and $Pr = 0.7$ is given in Fig. 4. The radial temperature profiles are nearly similar in the boundary-layer region, $0° \leq \theta \leq 120°$. At larger angles the turning of the flow to form the plume greatly alters the temperature distribution. The thermal-boundary layer thickness is essentially infinite near the center of the plume.

Local heat-transfer coefficients are shown as a function of angle and Rayleigh number for $Pr = 0.7$ in Fig. 5. The numerical solution to the boundary-layer equations obtained by Merkin [12] is shown for comparison. The boundary-layer result may be the limiting case as $Ra \to \infty$ for laminar flow excluding the plume region. Even at $Ra = 10^7$ the difference between the present local heat transfer and the boundary-layer solution at the bottom of the cylinder, $\theta = 0$, is 9%. With the exception of the region near $\theta = 0$, the boundary layer may become turbulent before curvature can be neglected. The boundary-layer solution does not give an adequate prediction of the heat transfer for $\theta > 130°$. Here the development of the plume makes boundary-layer assumptions invalid.

Local heat-transfer coefficients at $Pr = 0.1$, 1.0 and 10.0 are given in Fig. 6 for $Ra = 10^4$. The boundary-layer solution obtained by Merkin [12] for $Pr = 1$ and the perturbation solution from Akagi [13] also at $Pr = 1$ are shown for comparison. The present results for all three Prandtl numbers parallel the boundary-layer solution when θ is small. The curve for $Pr = 0.1$ deviates from the boundary-layer trend near $\theta = 90°$ indicating that a wide plume is forming covering

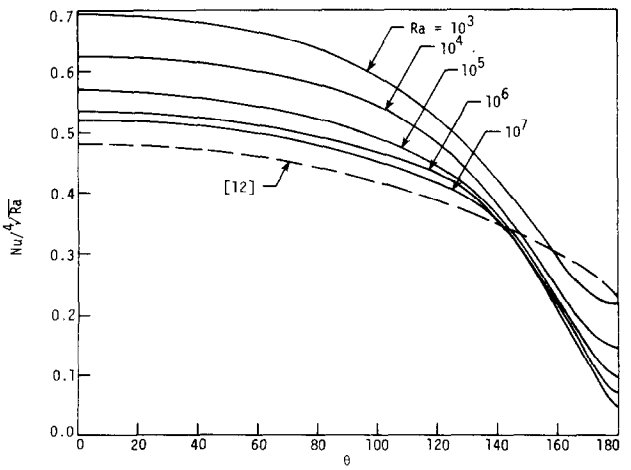

FIG. 5. Influence of Rayleigh number on local heat-transfer coefficients at $Pr = 0.7$.

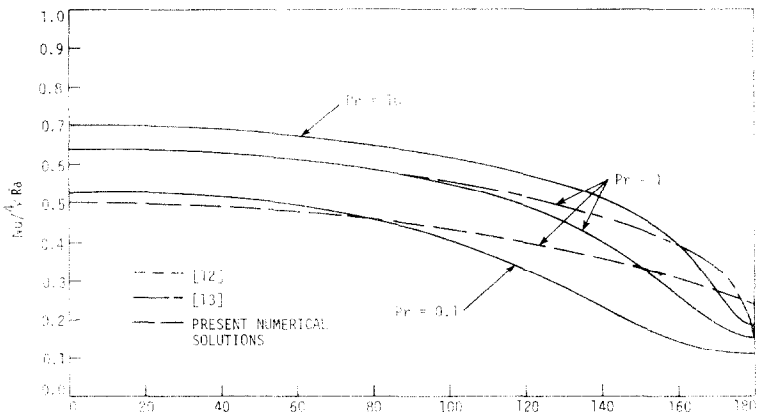

FIG. 6. Influence of Prandtl number on local heat-transfer coefficients at $Ra = 10^4$.

nearly the top half of the cylinder. The curve for $Pr = 10$ is roughly parallel to the boundary-layer curve until $\theta = 140°$ indicating the existence of a narrow plume above the cylinder. The boundary-layer solution for $Pr = 1$ gives heat-transfer coefficients that are considerably less than the present results except in the region of the plume, $150° \leq \theta \leq 180°$. Akagi's perturbation solution gives values almost identical to the present results for $0 \leq \theta \leq 90°$. At larger angles the agreement is not as good, indicating the breakdown of the boundary-layer solution that is used as the first term in his perturbation series.

EXPERIMENTAL VERIFICATION

A hollow copper cylinder, 3.56 cm in diameter and 20.3 cm long, was suspended from wires at each end in the beam of a Mach–Zehnder interferometer. Six thermocouples mounted in the horizontal cylinder measure the angular- and axial-temperature variations. An electric resistive element inside the tube heats the cylinder to the desired temperature. Expanded foam disks were added to thermally insulate the ends. Large pieces of rigid insulation formed a chamber approximately 80 cm across and 100 cm high. This helped damp out room air fluctuations although gaps were left near the top and bottom to allow the air to circulate freely past the cylinder.

The electric power to the heater was adjusted until the thermocouples measured a temperature difference of 32.5°C between the cylinder surface and the ambient air. A photograph of the infinite fringe pattern was taken on 35 mm film after conditions had remained stable for 30 min. The fringe pattern appeared symmetric about a vertical plane through the center of the cylinder. Analysis of the data indicated a Rayleigh number of 1.02×10^5 and a Prandtl number of 0.705. The film negative was analyzed on a toolmaker's microscope to measure the location of each half fringe shift every 15° around one side of the cylinder. The temperature of each fringe was calculated and the resulting local natural-convection heat-transfer coefficients determined.

Figure 7 is a comparison of the experimentally-obtained fringe pattern or isotherm distribution and the corresponding theoretical isotherms obtained from the numerical solution for $Ra = 10^5$ and $Pr = 0.7$. The agreement is very good, especially in the boundary-layer region. The temperature distributions in the plume compare favorably. However, the experimental-plume center-line temperature decreases

Table 1. Local and average heat-transfer coefficients from numerical solutions

		Nu							
Ra	Pr	$\theta = 0°$	30°	60°	90°	120°	150°	180°	$\overline{Nu}$
10^0	0.7	1.41	1.37	1.25	1.08	0.87	0.68	0.56	1.04
10^1	0.7	1.83	1.79	1.67	1.47	1.21	0.94	0.81	1.40
10^2	0.7	2.71	2.66	2.51	2.23	1.80	1.27	0.97	2.05
10^3	0.7	3.89	3.85	3.72	3.45	2.93	2.01	1.22	3.09
10^4	0.7	6.24	6.19	6.01	5.64	4.82	3.14	1.46	4.94
10^5	0.7	10.15	10.03	9.65	9.02	7.91	5.29	1.72	8.00
10^6	0.7	16.99	16.78	16.18	15.19	13.60	9.38	2.12	13.52
10^7	0.7	29.41	29.02	27.95	26.20	23.46	16.48	2.51	23.32
10^4	0.01	3.63	3.56	3.17	2.51	1.74	1.13	0.93	2.40
10^4	0.1	5.25	5.16	4.89	4.34	3.26	1.84	1.12	3.78
10^4	1.0	6.40	6.33	6.10	5.69	4.91	3.36	1.48	5.06
10^4	5.0	6.89	6.82	6.59	6.19	5.55	4.35	1.74	5.66
10^4	10.0	7.01	6.93	6.69	6.29	5.71	4.67	1.79	5.81

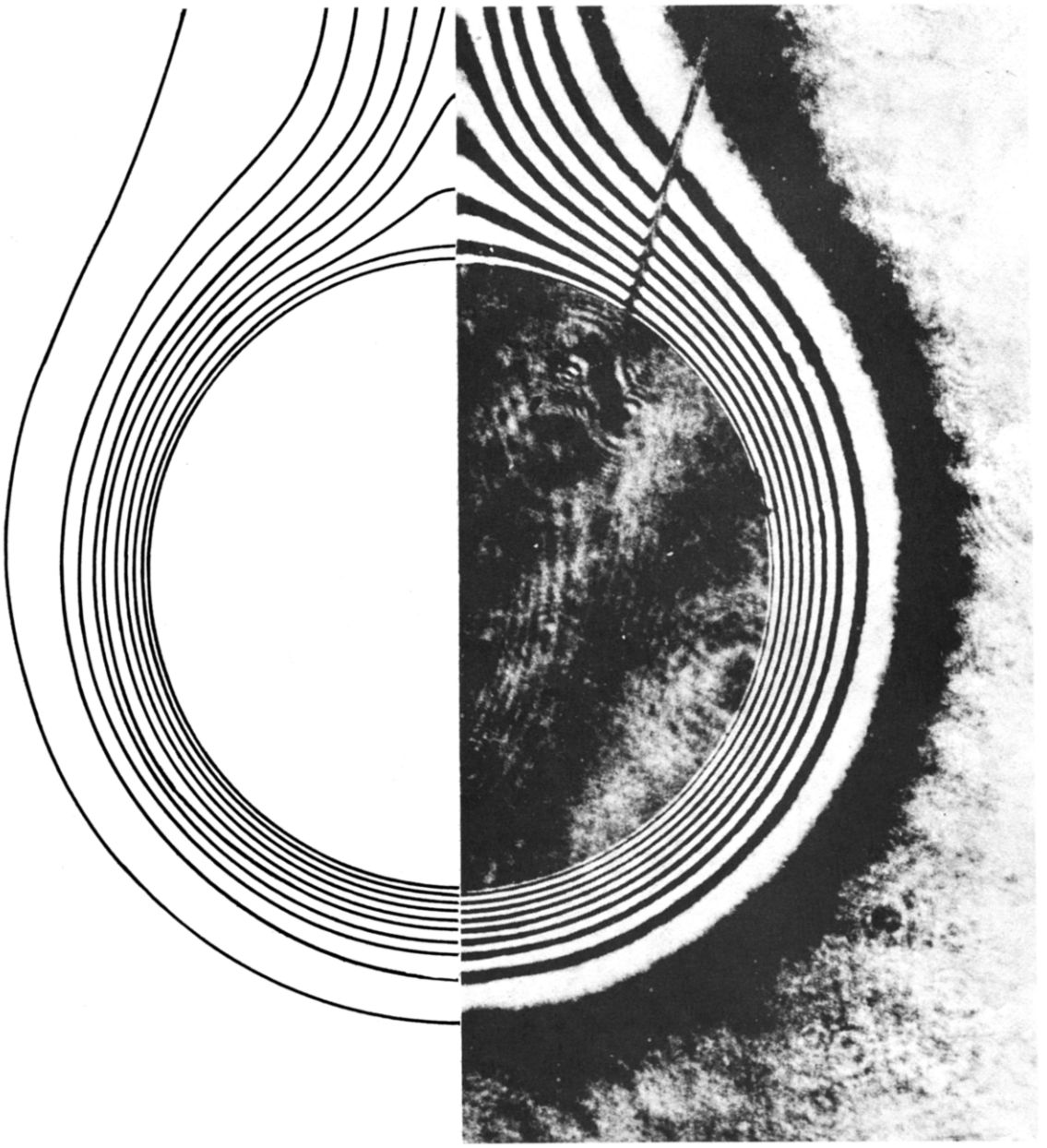

FIG. 7. Comparison of experimental and numerical isotherms for air, $Ra = 10^5$.

more rapidly than the prediction. This may be due to end effects in the experiment where axial velocities at the ends tend to make the plume neck down. Since the interferometer is producing axially-integrated values of the index of refraction or temperature, necking of the plume would result in a faster drop in observed temperature than in a strictly two-dimensional plume.

Comparison of the calculated angular velocity profile for $Ra = 10^5$, $Pr = 0.7$ and $\theta = 90°$ with experimental measurements is given in Fig. 8. The analytical result from Chiang and Kaye [7] for $\theta = 90°$ and $Pr = 0.7$ is given for comparison as being representative of the boundary-layer solutions. The measurements of Jodlbauer [19] agree with the present calculations. Those of Aihara and Saito [18] agree very well with the present results for $Y^* < 1$ but are closer to the boundary-layer solution for $Y^* > 2$.

Comparison of the calculated temperature distributions at $Ra = 10^5$, $Pr = 0.7$ and $\theta = 90°$ and 180° with experimental results is shown in Fig. 9. At $\theta = 90°$ the experimental values agree well with the numerical results. At the plume center line, $\theta = 180°$, the experimental results agree very well when $Y^* < 2$. At distances larger than this the agreement is not as good.

Experimental local heat-transfer coefficients for air agree very well with the present numerical results for $Ra = 10^5$, $Pr = 0.7$ as shown on Fig. 10. The boundary-layer curve obtained by Merkin [12] is shown for comparison.

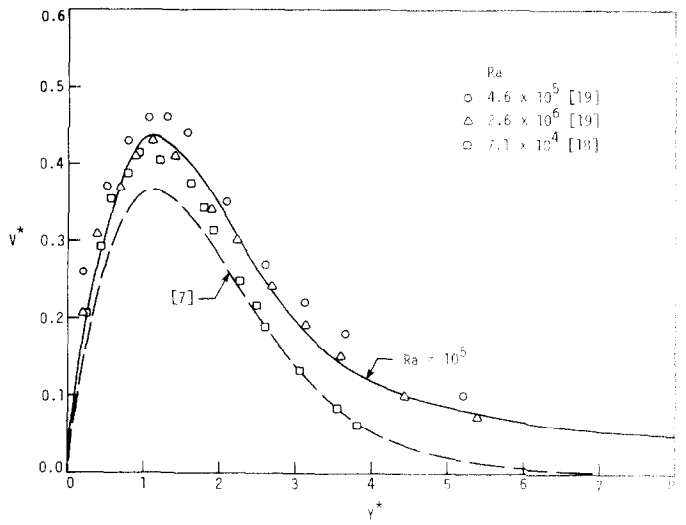

FIG. 8. Comparison of experimental and theoretical angular velocities for air at $\theta = 90^\circ$ near $Ra = 10^5$.

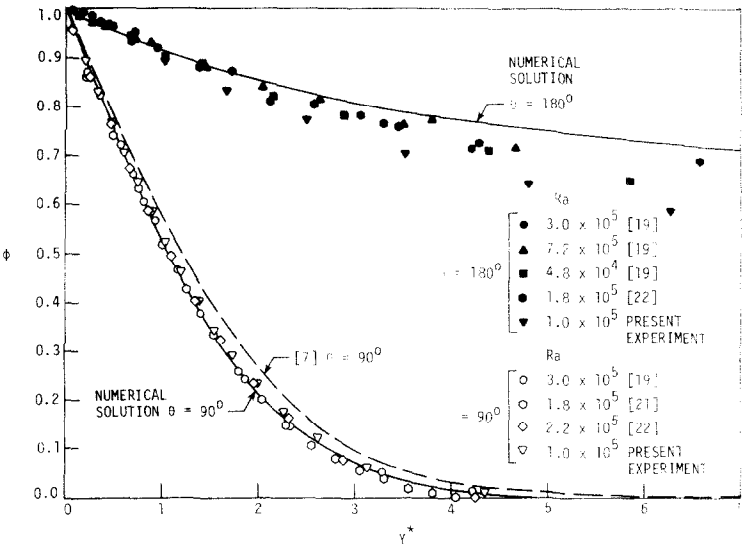

FIG. 9. Comparison of experimental and theoretical temperatures for air at $\theta = 90^\circ$ and 180° near $Ra = 10^5$.

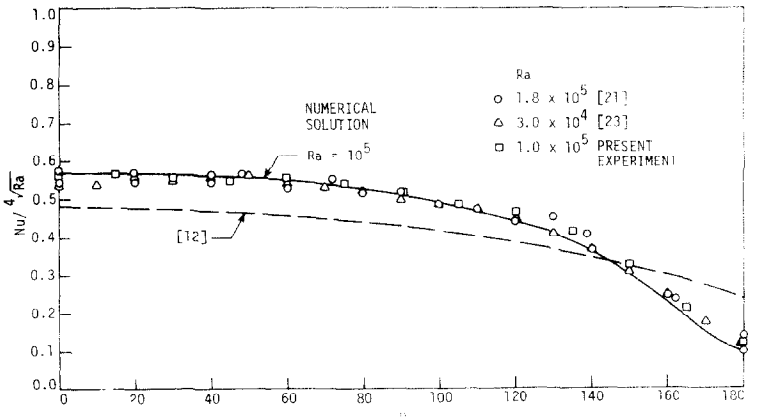

FIG. 10. Comparison of experimental and theoretical local heat-transfer coefficients for air near $Ra = 10^5$.

SUMMARY AND CONCLUSIONS

Solutions to the Navier–Stokes and energy equations have been obtained for natural-convection heat transfer from a horizontal isothermal cylinder. Results at small Rayleigh numbers approach natural convection from a line heat source. Boundary-layer conditions may be reached at the lower portion of the cylinder when the Rayleigh number becomes very large. Solutions to the laminar boundary-layer equations will not give accurate results at moderate values of the Rayleigh number because curvature effects are always present and boundary-layer approximations are invalid in the region of the plume. Experimentally determined velocities, temperatures and heat-transfer coefficients agree with the present numerical results.

Acknowledgement—The authors wish to acknowledge the University of Minnesota Computer Center for a grant of computer time, the National Science Foundation for support under Grant ENG-7721626, and partial support from the Engineering Research Institute, Iowa State University.

REFERENCES

1. V. T. Morgan, The overall convective heat transfer from smooth circular cylinders, *Adv. Heat Transfer* **11,** 199–264 (1975).
2. S. Nakai and T. Okazaki, Heat transfer from a horizontal circular wire at small Reynolds and Grashof numbers—I, *Int. J. Heat Mass Transfer* **18,** 387–396 (1975).
3. R. Hermann, Heat transfer by free convection from horizontal cylinders in diatomic gases, NACA TM 1366 (1954).
4. S. Ostrach, An analysis of laminar free convection flow and heat transfer about a flat plate parallel to the direction of the generating body force, NACA TR 1111 (1953).
5. H. J. Merk and J. A. Prins, Thermal convection in laminar boundary layers, Parts I, II and III, *Appl. Scient. Res.* **4A,** 11–24, 195–206, 207–224 (1953–54).
6. S. Levy, Integral methods in natural convection flow, *J. Appl. Mech.* **22,** 515–522 (1955).
7. T. Chiang and J. Kaye, On laminar free convection from a horizontal cylinder, *Proceedings of the Fourth National Congress of Applied Mechanics,* pp. 1213–1219 (1962).
8. D. A. Saville and S. W. Churchill, Laminar free convection in boundary layers near horizontal cylinders and vertical axisymmetric bodies, *J. Fluid Mech.* **29,** 391–399 (1967).
9. L. Elliott, Free convection on a two-dimensional or axisymmetric body, *Q. J. Mech. Appl. Math.* **23,** 153–162 (1970).
10. F. N. Lin and B. T. Chao, Laminar free convection over two-dimensional and axisymmetric bodies of arbitrary contour, *J. Heat Transfer* **96,** 435–442 (1974).
11. J. H. Merkin, Free convection boundary layer on an isothermal horizontal cylinder, ASME Paper No. 76-HT-16 (1976).
12. J. H. Merkin, Free convection boundary layers on cylinders of elliptic cross section, *J. Heat Transfer* **99,** 453–457 (1977).
13. S. Akagi, The effect of curvature on free convection around a horizontal cylinder, *Trans. JSME* **31,** 1327–1335 (1965).
14. J. A. Peterka and P. D. Richardson, Natural convection from a horizontal cylinder at moderate Grashof numbers, *Int. J. Heat Mass Transfer* **12,** 749–752 (1969).
15. A. S. Gupta and I. Pop, Effects of curvature on unsteady free convection past a circular cylinder, *Physics Fluids* **20,** 162–163 (1977).
16. T. H. Kuehn, Natural convection heat transfer from a horizontal circular cylinder to a surrounding cylindrical enclosure, Ph.D. Thesis, University of Minnesota, MN (1976).
17. A. W. Schorr and B. Gebhart, An experimental investigation of natural convection wakes above a line heat source, *Int. J. Heat Mass Transfer* **13,** 557–571 (1970).
18. T. Aihara and E. Saito, Measurement of free convection velocity field around the periphery of a horizontal torus, *J. Heat Transfer* **94,** 95–98 (1972).
19. K. Jodlbauer, Das Temperatur- und Geschwindigkeitsfeld um ein Geheiztes Rohr bei freier Konvektion, *Forschung Ver. Dt. Ing.* **4,** 158–172 (1933).
20. N. E. Hardwick and E. K. Levy, Study of the laminar free-convection wake above an isothermal vertical plate, *J. Heat Transfer* **95,** 289–294 (1973).
21. D. A. Didion and Y. H. Oh, A quantitative grid-Schlieren method for temperature measurement in a free convection field, Technical Report No. 1, The Catholic University of America, Washington, DC (1966).
22. G. Havener and R. J. Radley, Jr., Quantitative measurements using dual hologram interferometry, Aerospace Research Laboratories Report 72-0085 (1972).
23. E. R. G. Eckert and E. E. Soehngen, Studies on heat transfer in laminar free convection with the Zehnder–Mach interferometer, Wright-Patterson AFB Technical Report 5747, ATI-44580 (1948).

SOLUTION NUMERIQUE DES EQUATIONS DE NAVIER–STOKES POUR LA CONVECTION LAMINAIRE NATURELLE AUTOUR D'UN CYLINDRE CIRCULAIRE, HORIZONTAL ET ISOTHERME

Résumé—La convection thermique laminaire, naturelle autour d'un cylindre horizontal, isotherme est étudiée en résolvant les équations de Navier–Stokes et d'énergie à partir d'une procédure numérique elliptique. Des résultats sont obtenus pour $10^0 \leqslant Ra \leqslant 10^7$. L'écoulement approche celui de la convection naturelle à partir d'une source de chaleur linéaire quand $Ra \to 0$ et celui de la couche limite laminaire quand $Ra \to \infty$. Des solutions de couche limite ne décrivent pas correctement l'écoulement et le transfert thermique aux valeurs faibles ou modérées de Ra parce qu'elles négligent les effets de courbure et les hypothèses de rupture de la couche limite dans la région du panache. On obtient un accord avec les résultats expérimentaux.

NUMERISCHE LÖSUNG DER NAVIER-STOKES-GLEICHUNGEN FÜR LAMINARE NATÜRLICHE KONVEKTION AN EINEM HORIZONTALEN ISOTHERMEN KREISZYLINDER

Zusammenfassung—Es wurde die Wärmeübertragung durch laminare natürliche Konvektion an einem horizontalen isothermen Zylinder untersucht, indem die Navier-Stokes- und Energiegleichungen unter Verwendung eines elliptischen numerischen Verfahrens gelöst wurden. Ergebnisse wurden für $10^0 \leqslant Ra \leqslant 10^7$ erhalten. Für $Ra \to 0$ nähert sich die Strömung der natürlichen Konvektion einer linienförmigen Wärmequelle und für $Ra \to \infty$ einer laminaren Grenzschichtströmung an. Grenzschichtlösungen beschreiben die Strömung und Wärmeübertragung bei kleinen oder mittleren Werten von Ra nicht ausreichend, und zwar wegen der Vernachlässigung der Krümmungseinflusse und weil die Grenzschichtannahmen in Bereich der Schlieren nicht zutreffen. Gute Übereinstimmung mit experimentellen Ergebnissen wurde erzielt.

ЧИСЛЕННОЕ РЕШЕНИЕ УРАВНЕНИЙ НАВЬЕ–СТОКСА ДЛЯ ЛАМИНАРНОЙ ЕСТЕСТВЕННОЙ КОНВЕКЦИИ У ГОРИЗОНТАЛЬНОГО ИЗОТЕРМИЧЕСКОГО КРУГЛОГО ЦИЛИНДРА

Аннотация — Теплообмен при ламинарной конвекции от горизонтального изотермического цилиндра исследуется методом численного решения уравнений Навье–Стокса и энергии. Результаты получены в диапазоне чисел Ra от 10^0 до 10^7. При $Ra \to 0$ течение приобретает характер свободноконвективного потока от линейного источника тепла, а при $Ra \to \infty$ — ламинарного течения в пограничном слое. Установлено, что при низких и умеренных значениях числа Ra течение и теплоперенос нельзя адекватно описать с помощью решения в приближении пограничного слоя из-за пренебрежения эффектами кривизны и нарушения допущений пограничного слоя в области свободноконвективного восходящего движения. Получено хорошее совпадение с экспериментальными данными.